Electrochemistry Communications 128 (2021) 107057

Contents lists available at ScienceDirect

Electrochemistry Communications

journal homepage: www.elsevier.com/locate/elecom

Short Communication

Electrodeposition of a CoNiCu medium-entropy alloy in a water-in-oil emulsion

Yuki Murakami, Yuki Maeda, Atsushi Kitada, Kuniaki Murase, Kazuhiro Fukami *

Department of Materials Science and Engineering, Kyoto University, Kyoto 606-8501, Japan

ARTICLE INFO

Keywords:
Ternary alloy
Medium-entropy alloy
Electrodeposition
Emulsion
Water-in-oil

ABSTRACT

A medium-entropy alloy (MEA) of CoNiCu with a face-centered cubic structure was successfully obtained by electrochemical deposition. To achieve a nearly equiatomic composition, a water-in-oil emulsion was used as the solution for electrodeposition. Since the water droplets in the emulsion tended to be destroyed within 10 min under electrolysis, the emulsion was periodically irradiated ultrasonically to maintain its emulsified state in order to obtain a continuous film by electrodeposition. Characterization of the film deposited under a constant potential reveals that the deposit is metallic with a face-centered cubic structure. The nearly equiatomic composition suggests that the deposit is a CoNiCu medium-entropy alloy.

1. Introduction

Multicomponent alloys containing five or more elements with a nearly equiatomic ratio have attracted much attention in terms of their mechanical properties since they are expected to exhibit excellent strength and toughness. These alloys are called *high-entropy alloys* (HEAs) [1,2]. They are generally produced by casting; however, other fabrication approaches such as laser cladding [3,4] and the carbothermal shock method [5,6] have been thoroughly investigated. *Medium-entropy alloys* (MEA), which contain less than five elements with a nearly equiatomic ratio, have also been objects of intensive study [7,8].

Arranging for the metal composition to be a nearly equiatomic ratio is critical to the production of HEAs and MEAs with excellent properties. However, such control of the composition is difficult using conventional electrodeposition techniques due to the differences in the redox potential of each constituent metal. Recently, Glasscott et al. reported that high-entropy metallic glass (amorphous) nanoparticles can be deposited electrochemically using a water-in-oil emulsion as an electrolytic solution [9]. They used 1,2-dichloroethane (DCE) as an oil phase and dissolved metal salts in the water phase to form a water-in-oil emulsion. Tuning the concentration ratio of the salts in the water droplets directly controlled the composition of the deposited nanoparticles. However, two issues remain from a structural materials standpoint. First, the deposit must have a crystalline structure. HEAs and MEAs with face-centered cubic (fcc) structures in particular are expected to show excellent mechanical properties [10,11]. Second, a continuous and thick film must be deposited instead of nanoparticles. Additionally, the mechanism of electrodeposition in the water-in-oil emulsion should be clarified and discussed in detail, although some studies of emulsions have already been reported from an electrochemical viewpoint [12,13].

In the present paper, we report the successful production of a crystalline and nearly equiatomic CoNiCu MEA film by electrodeposition using a water-in-oil emulsion. Based on the LSV measurements, the potentials at which hydrogen evolution and the cathodic decomposition of DCE occur were clarified. Using this information, we chose an applied potential at which water droplets reacted, but the DCE did not, in order to produce a continuous film as a deposit. Characterization of the deposited film revealed that it is a crystalline metal with a nearly equiatomic composition. We believe that this study is a milestone in the electrochemical production of continuous films of MEAs and HEAs using water-in-oil emulsions.

2. Experimental

All the chemicals used in this study were of analytical grade. We initially prepared a solution containing DCE (Nacalai Tesque Inc.) with 0.1 M $(C_4H_9)_4NClO_4$ (Nacalai Tesque Inc.) (M = mol L^{-1}) and an aqueous solution containing 10 mM $CoCl_2{\cdot}6H_2O$ (FUJIFILM Wako Pure Chemicals), 20 mM $NiCl_2{\cdot}6H_2O$ (FUJIFILM Wako Pure Chemicals), and 10 mM $CuCl_2{\cdot}2H_2O$ (Nacalai Tesque Inc.). Additionally, we added sodium dodecyl sulfate (SDS, Aldrich) and H_3BO_3 (FUJIFILM Wako Pure Chemicals) into the aqueous solution to produce concentrations of 100

* Corresponding author.
E-mail address: fukami.kazuhiro.2u@kyoto-u.ac.jp (K. Fukami).

https://doi.org/10.1016/j.elecom.2021.107057
Received 22 April 2021; Received in revised form 19 May 2021; Accepted 25 May 2021
Available online 28 May 2021

mM and 400 mM, respectively. The concentration of SDS was chosen so that it is much higher than its critical micelle constant (8.5 mM) [14]. By contrast, the concentration of H_3BO_3 was selected to be similar to conventional electrodeposition systems in aqueous solutions [15]. H_3BO_3, as a buffering agent, suppresses the increase in pH in the water droplets under electrolysis, while SDS stabilizes the water droplets as an emulsifier. We found that a non-negligible amount of hydroxides were precipitated during electrodeposition in an emulsion without pH buffering, and the utilization of an emulsifier is necessary because of the unstable nature of the water-in-oil emulsion formed between DCE and the aqueous solution. Then 10 mL of the DCE solution and 60 μL of the aqueous solution were mixed using a high-intensity ultrasonic processor (Vibra cell 75186) at an output power of 130 W. The pH of the aqueous solution was adjusted to 1 using hydrochloric acid (Nacalai Tesque Inc.). The size distribution of the water droplets was measured by dynamic light scattering (DLS; Otsuka Electronics, ELSZ-2Plus). The electrochemical measurements were carried out with a potentiostat (Biologic, SP-50) using a three-electrode cell with a mechanically polished molybdenum (Mo) sheet as the working electrode, which was placed horizontally at the bottom of the cell, a platinum rod as the counter electrode, and Ag|AgCl in 1.0 M NaCl as the reference electrode. All the potentials in this study are specified relative to the reference electrode. The cell geometry has been reported elsewhere [16]. The volume of the emulsion was roughly 10 mL, and the disk electrode had an area of 0.785 cm^2 with a diameter of 10 mm. The reason why a Mo sheet was used as the substrate is that the characterization of the CoNiCu MEA using a Mo substrate is simpler since the peaks of the energy-dispersive X-ray (EDS) spectra of Mo as well the X-ray diffraction (XRD) results are well separated from those of Co, Ni, and Cu.

To characterize the deposits, field-emission transmission electron microscopy (STEM; JEOL, JEM-2100F) together with EDS, XRD (PANalytical, X'Pert PRO Alpha-1 with Cu Kα 1.542 Å), and X-ray photoelectron spectroscopy (XPS; JEOL, JPS-9010TRX) were employed. TEM samples were prepared by the focused ion beam system (FIB; Hitachi, FB2200).

3. Results and discussion

Firstly we conducted some electrochemical measurements. Fig. 1(a) shows three linear sweep voltammograms (LSVs). One LSV was recorded in the 0.1 M $(C_4H_9)_4NClO_4$ DCE solution. The other two were recorded in the water-in-oil emulsions with and without metal salts. The LSV in 0.1 M $(C_4H_9)_4NClO_4$ DCE solution shows two cathodic waves starting roughly from − 1.0 V and − 2.0 V. DCE contained a non-negligible amount of water because it was not distilled before use. Therefore, both DCE and water should undergo reduction in the DCE solution. The reduction at − 1.0 V is assigned to water decomposition, while that at − 2.0 V originates from DCE decomposition because water has a much narrower electrochemical window than DCE.

The LSV in the emulsion without metal salts is similar to that in the DCE solution, except that the absolute value of the reduction current increases in the emulsion due to an increase in water content. When using the emulsion with the metal salts, the LSV slightly changes in the potential region between − 1.0 V and − 1.3 V. The reduction current density increases slightly due to metal deposition from the water droplets in the emulsion. Additionally, the reduction of water and DCE were detected in the LSV since an increase in the reduction current density was observed at both − 1.4 V and − 2.0 V. To effectively promote the electrodeposition of a CoNiCu MEA, the decomposition of DCE should be suppressed as much as possible, while the overpotential should be as high as possible. Consequently, we chose − 1.5 V as the applied potential for MEA film deposition. The effect of ion concentration on the reduction current density has been difficult to determine so far. The estimated concentration of metal ions in the emulsion (a mixture of 10 mL of DCE and 60 μL of the aqueous solution) was as low as 0.24 mM, and most of the reduction current density originates from hydrogen evolution, not from metal deposition.

Fig. 1(a) suggests that the water droplets tend to decompose at − 1.5 V since water is reduced to hydrogen. Thus, the lifetime of the water droplets in the emulsion may affect the electrodeposition. Fig. 1(b) shows the change in the water droplet size with time by measuring the droplet size with and without electrolysis. After 10 min without electrolysis, the average size increases from ~ 350 nm to ~ 800 nm. By contrast, the emulsion is unstable under electrolysis. Indeed, the DLS results indicate that the water droplet size greatly increases. After 10 min of electrolysis, the average diameter is greater than 1000 nm. This suggests that continuous ultrasonic irradiation is necessary to maintain the emulsified state during electrodeposition. The reason why the water droplets were destabilized under electrolysis is not clear. Hydrogen evolution from the three-phase boundary may play some role in the destabilization. The other possibility may be related to how the water droplets behave when they attach to and detach from the electrode surface. These issues must be investigated to understand this electrodeposition method in detail and we plan to address them in a future study.

Based on the above results, potentiostatic electrodeposition at − 1.5 V was carried out under periodic ultrasonic irradiation (turning on/off every 5 s). Fig. 1(c) shows the time development of the current density for electrodeposition. The cathodic current density fluctuates intensively with the on/off cycling of the ultrasonic irradiation. The emulsion maintained its emulsified state during electrodeposition under this periodic irradiation. During electrodeposition under periodic ultrasonic irradiation, 40 μL of an aqueous solution containing the metal salts was added every 10 min to avoid the depletion of metal ions, and to ensure that the concentrations of metal ions are kept nearly constant. Although we prepared the aqueous solution so that the total concentration of metal ions was 40 mM, the apparent concentration of metal ions estimated based on the volume of the emulsion was 0.24 mM, which is quite low compared with conventional electrodeposition in aqueous solutions. Thus, it is important to periodically supply metal ions to the emulsion. Immediately after the additional injection of the aqueous solution, the current density increases slightly. However, it settles down to nearly the same current density after a few cycles of ultrasonic irradiation. The current density tends to increase gradually (Fig. 1c). This indicates that the surface roughness increases during electrodeposition. After 3 h of electrodeposition, a continuous film is obtained. Without ultrasonic irradiation, a small number of nanoparticles were deposited, but continuous films were never obtained. After the deposition, the emulsion became dark as the deposit became mechanically detached and formed a suspension. Also, the amount of deposit is still small; therefore, it is difficult to discuss the electrodeposition process quantitatively.

The deposited film was characterized by XRD (Fig. 2a). Two diffraction peaks, which do not exactly match the patterns of pure metallic Co, Ni, or Cu, appear. The peaks at 44.04° and 51.16° are respectively assigned to fcc 111 and 200 reflections. There are no diffraction peaks, except those of the Mo substrate. Since the diffraction pattern of our sample is highly symmetric and cannot be reproduced using the diffraction patterns of the pure metals, especially for 200 diffraction, it is clear that the sample is not a mixture of pure Co, Ni, and Cu. In the case of binary alloys, the diffraction pattern appears to be between those of the two pure metals. However, even considering binary alloys, the symmetric diffraction of our sample cannot be reproduced. Furthermore, the nano-beam electron diffraction (NBD) from a single crystal particle of the deposit was measured, and the lattice spacings for 111 and 200 diffractions derived from XRD and NBD were compared. The values of the lattice spacings matched each other. From this result, together with the uniform distribution of Co, Ni, and Cu, it was concluded that the deposit was not a mixture but a MEA.

The cross-section of the sample was then characterized by STEM as shown in Fig. 2(b), indicating that the film is ~ 350 nm thick. The EDS mappings of Co, Ni, and Cu confirm that these elements are distributed uniformly within the film. Note that a layered structure is observed in

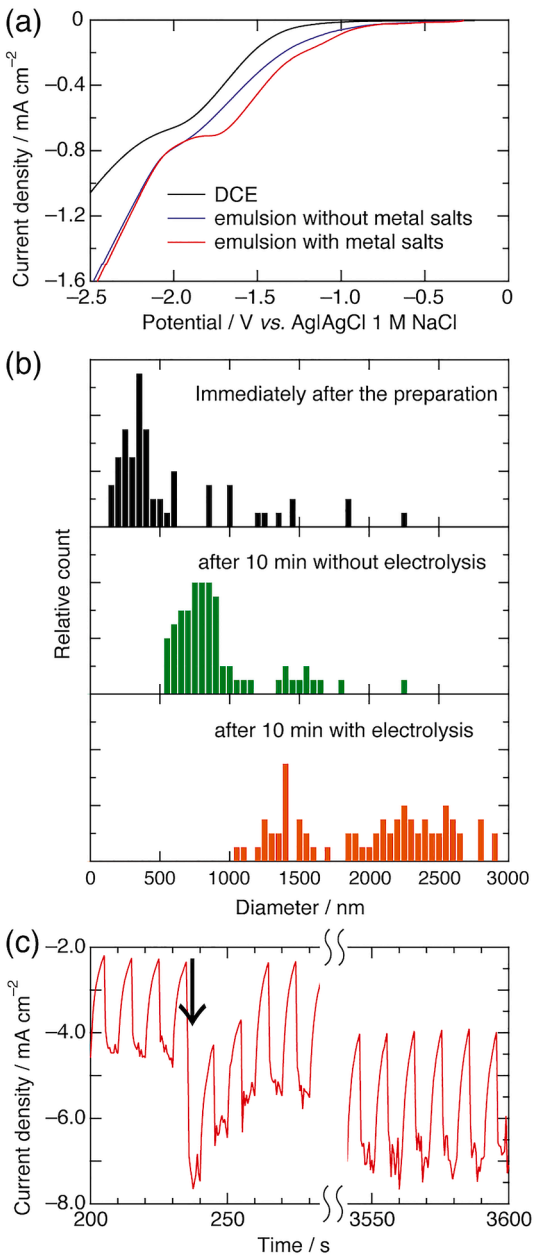

Fig. 1. (a) LSVs measured in 0.1 M $(C_4H_9)_4NClO_4$ of a DCE solution (black), a water-in-oil emulsion without metal salts (blue), and a water-in-oil emulsion with metal salts (red). Scan rate is 50 mV s^{-1}. (b) Size distribution of the water droplets in the emulsion immediately after preparation (top), after 10 min without electrolysis (middle), and after 10 min with electrolysis (bottom). (c) Time development of the current density during electrodeposition. Deposition is carried out at − 1.5 V vs. Ag|AgCl in 1.0 M NaCl under periodic ultrasonic irradiation in 5-second on/off cycles. The arrow indicates the addition of a small amount of the aqueous solution. (For interpretation of the references to colour in this figure legend, the reader is referred to the web version of this article.)

the cross-section, but this is attributed to the addition of a small amount of the aqueous solution to maintain the emulsified state, which caused a slight change in the deposition behavior. As previously mentioned, the composition fluctuates slightly when the aqueous solution is added.

The atomic ratio of Co, Ni, and Cu is roughly estimated based on the EDS results. The best composition occurs at 30.0:33.6:33.2. This composition is observed near the Mo substrate. Note that small amounts of O, W (deposition on the top surface before the FIB processing), and Mo were also detected. The depth profile of EDS in Fig. 2(c) suggests that the composition of the deposit is relatively constant from the bottom to the top. It should be noted that the total concentration of metal ions was kept at 40 mM in the water phase following the previous study by Glasscott et al. [9]. Indeed, we tried several combinations of the concentrations of Co, Ni, and Cu and found that the amount of Ni in the deposited film was slightly smaller than Co and Cu when an equimolar mixture was used. Therefore, in order to obtain the targeted composition of the alloy, the concentration of the nickel salt was set as double that of the other two salts.

It should be noted why the concentration of the Ni salt needs to be higher than the other two. We measured LSVs in aqueous solutions containing one of the metal salts. From these results, it became clear that the charge transfer resistance of Ni electrodeposition was quite high compared with that of the other two metals. Thus, it is possible that Co and Cu electrodeposition can reach the diffusion limit, while Ni electrodeposition may not. In this case, a higher concentration of the Ni salt is necessary. In our experiments, we found that doubling the

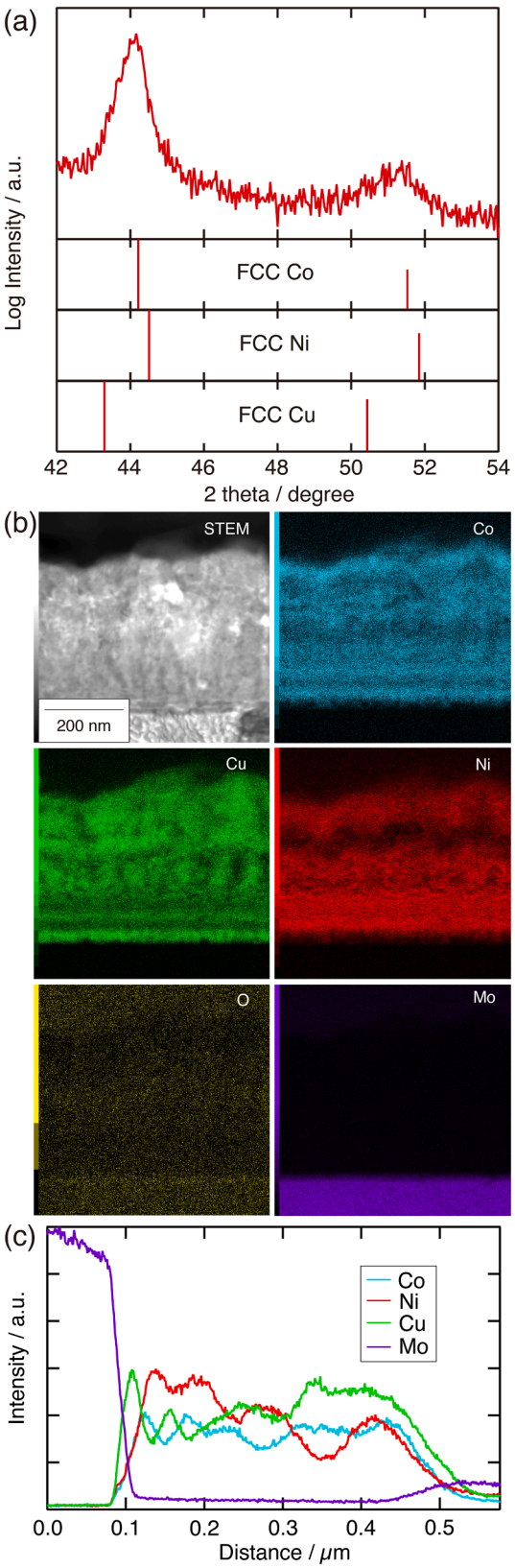

Fig. 2. (a) XRD pattern of the film deposited at − 1.5 V vs. Ag|AgCl in 1.0 M NaCl. Metallic Co, Ni, and Cu are shown as reference patterns. (b) STEM image and the corresponding EDS mappings of Co, Ni, Cu, Mo, and O at the cross-section of the film. (c) Depth profile of the elements measured by EDS.

concentration of the Ni salt gave the best result in producing the desired MEA.

To confirm that the deposit is an MEA, the oxidation state must be characterized. Fig. 3(a-d) show the XPS spectra of Co 2p3/2, Ni 2p3/2, Cu 2p3/2, and Cu LMM at the surface. At the surface of the deposit, Co and Ni are detected as oxides. The spectrum of Cu 2p3/2 suggests that

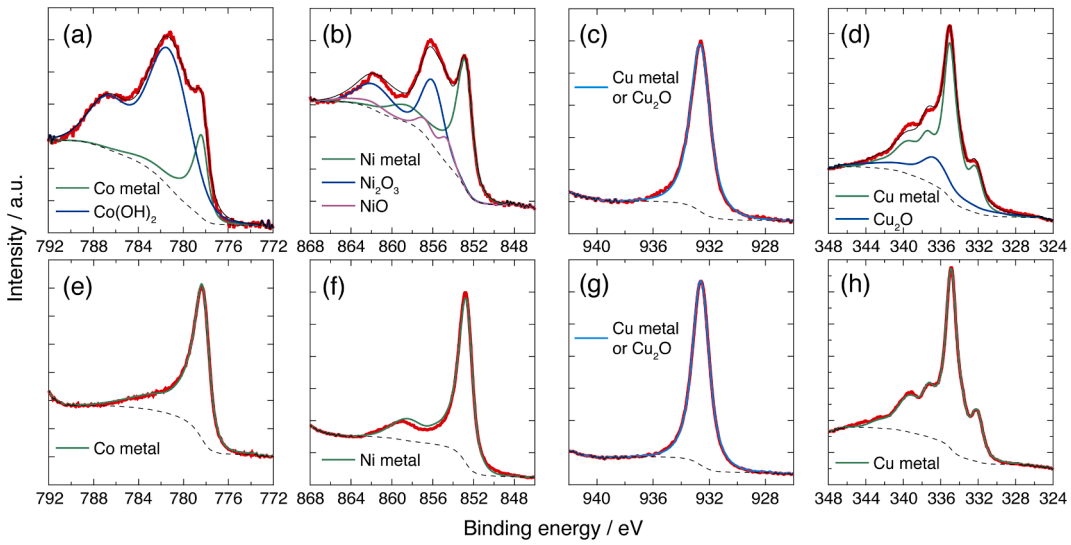

Fig. 3. XPS spectra. (a,e) Co 2p3/2, (b,f) Ni 2p3/2, (c,g) Cu 2p3/2, and (d,h) Cu LMM measured with the deposit. (a–d) and (e–h) show the spectra at the surface and after etching with Ar for 150 s, respectively. Red solid (thick), black solid (thin), and black dotted curves in the spectra indicate the experimental data, fitted curves, and the background, respectively. (For interpretation of the references to colour in this figure legend, the reader is referred to the web version of this article.)

CuO is not formed; however, it is impossible to distinguish whether metallic Cu or Cu_2O is present on the surface. Therefore, we analysed the Auger peak between the L and M shells denoted as Cu LMM. The spectrum of Cu LMM clearly suggests the formation of Cu_2O. These results demonstrate that the surface of the deposit is partially oxidized.

Etching for 150 s with Ar changed the spectrum (Fig. 3e-h). The results after Ar etching clearly indicate that the deposit is metallic. Thus, the surface oxide may form spontaneously in the air. In fact, the backgrounds measured before and after Ar etching were almost the same, meaning that the signals of $Co(OH)_2$ and the nickel oxides were relatively weak. Based on these results, we conclude that the deposit is a CoNiCu MEA.

Finally, the effect of the hydrophobicity of the substrate should be discussed. We also conducted the MEA electrodeposition on a gold electrode. Again, on the gold electrode, electrodeposition did not proceed without ultrasonication, while a continuous film of the CoNiCu MEA was deposited under ultrasonication. This suggests that the less-hydrophobic surface tends to be covered with a sort of "thin" aqueous layer when the water droplets attach to the surface, and this thin aqueous layer suppresses electrodeposition of the MEA. Although it is true that a hydrophobic substrate is advantageous for the electrodeposition of high-entropy "nanoparticles" [9], the utilization of a hydrophobic substrate is not the optimum strategy for obtaining continuous films of MEAs. This is because the electrodeposition of such alloys is expected to self-terminate once the hydrophobic (original) surface is covered with the deposit, whose surface is less hydrophobic. Thus, to obtain continuous films of HEAs and MEAs, ultrasonic irradiation is more effective than the utilization of a hydrophobic substrate.

4. Conclusions

This study examined the electrodeposition of CoNiCu MEA. A water-in-oil emulsion formed with an aqueous solution containing metal salts and DCE yielded an equiatomic CoNiCu deposit. Based on the electrochemical measurements, the applied potential for electrodeposition was chosen to be − 1.5 V as this was sufficient to enhance the reaction of the water droplets in the emulsion without promoting the decomposition of DCE. DLS measurements clarified that the water droplets were destroyed during electrodeposition. Consequently, continuous ultrasonic irradiation was necessary for a film to be deposited. Characterization of the deposit by XRD, STEM, and XPS indicated that the deposit was an equiatomic CoNiCu, i.e. a MEA.

Electrodeposition in a water-in-oil emulsion is a promising strategy for fabrication of MEA coatings. The successful production of a continuous film during electrodeposition of the MEA is critical for practical applications. This electrodeposition mechanism should be applicable not only to MEA coatings but also to HEAs. It is believed that this study represents a milestone in studies of MEAs and HEAs based on electrochemistry.

Declaration of Competing Interest

The authors declare that they have no known competing financial interests or personal relationships that could have appeared to influence the work reported in this paper.

Acknowledgments

This work was supported by a JSPS Grant-in-Aid for Scientific Research B (Grant Number 21H01670; K.F.) and a Grant-in-Aid for JSPS Fellows (Grant Number 21J14738; Y. Maeda).

References

[1] J.W. Yeh, S.K. Chen, S.J. Lin, J.Y. Gan, T.S. Chin, T.T. Shun, C.H. Tsau, S.Y. Chang, Nanostructured high-entropy alloys with multiple principal elements: Novel alloy design concepts and outcomes, Adv. Eng. Mater. 6 (2004) 299–303.
[2] J.-W. Yeh, Alloy design strategies and future trends in high-entropy alloys, JOM 65 (12) (2013) 1759–1771.
[3] J. Liu, H. Liu, P. Chen, J. Hao, Microstructural characterization and corrosion behaviour of $AlCoCrFeNiTi_x$ high-entropy alloy coatings fabricated by laser cladding, Surf. Coat. Technol. 361 (2019) 63–74.
[4] Z. Tian, Y. Zhao, Y. Jiang, H. Ren, C. Qin, Investigation of microstructure and properties of $FeCoCrNiAlMo_x$ alloy coatings prepared by broadband-beam laser cladding technology, J. Mater. Sci. 55 (10) (2020) 4478–4492.
[5] H. Xie, F. Chen, A. Nie, T. Pu, M. Rehwoldt, D. Yu, Carbothermal shock synthesis of high-entropy-alloy nanoparticles, Science 359 (2018) 1489–1494.
[6] P. Xie, Y. Yao, Z. Huang, Z. Liu, J. Zhang, T. Li, G. Wang, R. Shahbazian-Yassar, L. Hu, C. Wang, Highly efficient decomposition of ammonia using high-entropy alloy catalysts, Nat. Commun. 10 (2019) 4011.
[7] F. Cao, P. Munroe, Z. Zhou, Z. Xie, Microstructure and mechanical properties of a multilayered CoCrNi / Ti coating with varying crystal structure, Surf. Coat. Technol. 350 (2018) 596–602.
[8] Y. Cai, Y. Chen, Z. Luo, F. Gao, L. Li, Manufacturing of $FeCoCrNiCu_x$ medium-entropy alloy coating using laser cladding technology, Mater. Des. 133 (2017) 91–108.

[9] M.W. Glasscott, A.D. Pendergast, S. Goines, A.R. Bishop, A.T. Hoang, C. Renault, J. E. Dick, Electrosynthesis of high-entropy metallic glass nanoparticles for designer, multi-functional electrocatalysis, Nat. Commun. 10 (2019) 2650.
[10] T. Bhattacharjee, I.S. Wani, S. Sheikh, I.T. Clark, T. Okawa, S. Guo, P. P. Bhattacharjee, Simultaneous strength-ductility enhancement of a nano-lamellar $AlCoCrFeNi_{2.1}$ eutectic high entropy alloy by cryo-rolling and annealing, Sci. Rep. 8 (2018) 3276.
[11] S. Yoshida, T. Bhattacharjee, Y.u. Bai, N. Tsuji, Friction stress and Hall-Petch relationship in CoCrNi equi-atomic medium entropy alloy processed by severe plastic deformation and subsequent annealing, Scr. Mater. 134 (2017) 33–36.
[12] J. Yoshida, J. Chen, K. Aoki, Electrochemical coalescence of nitrobenzene | water emulsions, J. Electroanal. Chem. 553 (2003) 117–124.
[13] K. Aoki, M. Li, J. Chen, T. Nishiumi, Spontaneous emulsification at oil-water interface by tetraalkylammonium chloride, Electrochem. Commun. 11 (2) (2009) 239–241.
[14] S.S. Shah, N.U. Jamroz, Q.M. Sharif, Micellization parameters and electrostatic interactions in micellar solution of sodium dodecyl sulfate (SDS) at different temperatures, Colloids Surf. A 178 (1-3) (2001) 199–206.
[15] Z. Zhang, A. Kitada, K. Fukami, Z. Yao, K. Murase, Electrodeposition of an iron thin film with compact and smooth morphology using an ethereal electrolyte, Electrochim. Acta 348 (2020), 136289.
[16] K. Fukami, Y. Tanaka, M.L. Chourou, T. Sakka, Y.H. Ogata, Filling of mesoporous silicon with copper by electrodeposition from an aqueous solution, Electrochim. Acta 54 (8) (2009) 2197–2202.